EINDHOVEN UNIVERSITY OF TECHNOLOGY

Sub-5 nm patterning by directed self-assembly of oligo(Dimethylsiloxane) liquid crystal thin films

Citation for published version (APA):
Nickmans, K., Murphy, J. N., de Waal, S. A. J., Leclere, P., Doise, J., Gronheid, R., Broer, D. J., & Schenning, A. P. H. J. (2016). Sub-5 nm patterning by directed self-assembly of oligo(Dimethylsiloxane) liquid crystal thin films. *Advanced Materials*, *28*(45), 10068-10072. https://doi.org/10.1002/adma.201602891

DOI:
10.1002/adma.201602891

Document status and date:
Published: 07/12/2016

Document Version:
Publisher's PDF, also known as Version of Record (includes final page, issue and volume numbers)

Please check the document version of this publication:

• A submitted manuscript is the version of the article upon submission and before peer-review. There can be important differences between the submitted version and the official published version of record. People interested in the research are advised to contact the author for the final version of the publication, or visit the DOI to the publisher's website.
• The final author version and the galley proof are versions of the publication after peer review.
• The final published version features the final layout of the paper including the volume, issue and page numbers.

Link to publication

General rights
Copyright and moral rights for the publications made accessible in the public portal are retained by the authors and/or other copyright owners and it is a condition of accessing publications that users recognise and abide by the legal requirements associated with these rights.

• Users may download and print one copy of any publication from the public portal for the purpose of private study or research.
• You may not further distribute the material or use it for any profit-making activity or commercial gain
• You may freely distribute the URL identifying the publication in the public portal.

If the publication is distributed under the terms of Article 25fa of the Dutch Copyright Act, indicated by the "Taverne" license above, please follow below link for the End User Agreement:

www.tue.nl/taverne

Take down policy
If you believe that this document breaches copyright please contact us at:

openaccess@tue.nl

providing details and we will investigate your claim.

Download date: 19. Mar. 2025

ADVANCED MATERIALS
www.advmat.de
Materials Views
www.MaterialsViews.com

Sub-5 nm Patterning by Directed Self-Assembly of Oligo(Dimethylsiloxane) Liquid Crystal Thin Films

*Koen Nickmans, Jeffrey N. Murphy, Bas de Waal, Philippe Leclère, Jan Doise, Roel Gronheid, Dick J. Broer, and Albertus P. H. J. Schenning**

The sustained shrinking of device components is an embodiment of human progress that has led to an explosion of micro- and nanotechnologies. Block copolymer (BCP)-based nanopatterning has paved a strong foundation in nanotechnology including nanoporous membranes, patterned magnetic media, and nanolithography. At the heart of the nanopatterning lies the thin-film microphase separation of chemically distinct and thermodynamically immiscible polymer blocks into dense periodic structures (10–100 nm). To enable pattern transfer, the respective blocks must contain sufficient etching contrast and resistance, which is commonly achieved by introducing silicon into one block of the copolymer.[1] Among these materials, poly(styrene)-*b*-poly(dimethylsiloxane) (PS-*b*-PDMS) is the most widely investigated BCP in which the PS block is removed by oxygen plasma resulting in a silica-rich nanopattern.[2,3] The periodic structure depends on the overall degree of polymerization of the polymer blocks (N) and the Flory–Huggins interaction parameter (χ). The additional requirement that χN exceed 10.5 for microphase separation to occur has led to a surge in so-called high-χ, low-N block copolymers[4] that target nanopatterns with minimum periodicities and therefore maximum feature densities.[5,6] Unfortunately, an immiscibility-driven approach will not suffice when sub-5 nm periodicities are desired,[4] preventing extendibility to smaller dimensions. In addition, although the assembly of block copolymers can be directed within a photolithographic prepattern,[7] the formation of defect-free periodic structures remains a challenge.[8]

For sub-5 nm periodicities, monodisperse small molecules such as liquid crystals (LCs) have been proposed.[4] LCs can form similar phases as reported for block copolymers, such as smectic (lamellar) or discotic (cylindrical) morphologies.[9] Therefore, LCs could operate beyond the scaling limits of block copolymers for nanopatterning applications, provided they can bear substantial etch selectivity.

Liquid crystals have the advantage that they can be easily aligned into defect free structures, by for example shear,[10] photoalignment layers,[11] and mechanical alignment layers,[12] though these methods are not generally applicable for thin films. Exciting work has been performed on the confinement of liquid crystals in structures such as microchannels,[13] nanogrooves,[14] or nanopores,[15] but the directed self-assembly of thin films with sub-5 nm periodicities has not been reported.

In this work, we explore oligo(dimethylsiloxane) (ODMS) liquid crystals[10,16,17] as candidates for sub-5 nm nanopatterning. In these LCs, the volume fraction of flexible inorganic ODMS has been systematically varied in comparison to the organic mesogenic core, resulting in various sub-5 nm, hybrid organic/inorganic morphologies. We further examine the LC self-assembly in thin films and demonstrate the compatibility of the ODMS LCs with graphoepitaxy, where ordered nanopatterns are achieved without additional annealing.

Oligo(dimethylsiloxane) liquid crystals were prepared by coupling monodisperse oligo(dimethylsiloxane) hydrides[18] to an alkyl-terminated four-ring rigid core.[19] The molecular structure of the ODMS liquid crystals is depicted in **Scheme 1**, where n represents the length of the ODMS tail. ODMS tails consisting of 7 (n = 5), 11 (n = 9), and 15 (n = 13) dimethylsiloxane units were used, resulting in liquid crystals LC-14Si, LC-22Si, and LC-30Si, respectively. All LCs were purified and fully characterized (Supporting Information).

To investigate the LC phase behavior, the LCs were analyzed by polarized optical microscopy (POM) and differential scanning calorimetry (DSC). The POM images (**Figure 1**) show birefringent multidomains typical for liquid crystals and signify a correlation length of the nanostructures contained within the domains that is on the order of micrometers. DSC (Figure S2, Supporting Information) shows the presence of mesophases

K. Nickmans, Dr. J. N. Murphy, Prof. D. J. Broer, Prof. A. P. H. J. Schenning
Laboratory of Functional Organic Materials and Devices
Department of Chemical Engineering and Chemistry
Eindhoven University of Technology
P.O. Box 513, 5600 MB, Eindhoven, The Netherlands
E-mail: a.p.h.j.schenning@tue.nl

B. de Waal
Laboratory of Macromolecular Organic Chemistry
Department of Chemical Engineering and Chemistry
Eindhoven University of Technology
5600 MB, Eindhoven, The Netherlands

Dr. P. Leclère
Laboratory for Chemistry of Novel Materials
Center for Innovation and Research in Materials and Polymers (CIRMAP)
University of Mons (UMONS)
Place du Parc 20, B 7000 Mons, Belgium

J. Doise
Department of Electrical Engineering
K.U. Leuven
Kasteelpark Arenberg 10, B-3001 Leuven, Belgium

J. Doise, Dr. R. Gronheid
Imec vzw
Kapeldreef 75, B-3001 Leuven, Belgium

Prof. D. J. Broer, Prof. A. P. H. J. Schenning
Institute for Complex Molecular Systems
Eindhoven University of Technology
5600 MB, Eindhoven, The Netherlands

This is an open access article under the terms of the Creative Commons Attribution-NonCommercial License, which permits use, distribution and reproduction in any medium, provided the original work is properly cited and is not used for commercial purposes.

The copyright line for this article was changed on October 7, 2016 after original online publication

DOI: 10.1002/adma.201602891

 © 2016 The Authors. Published by WILEY-VCH Verlag GmbH & Co. KGaA, Weinheim

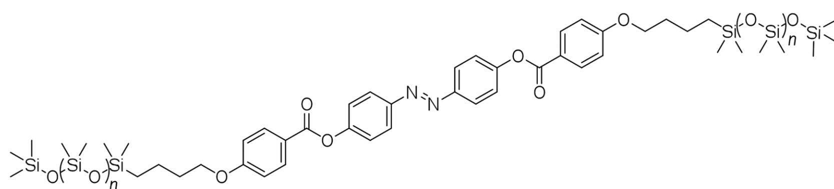

Scheme 1. Molecular structure of the ODMS liquid crystals, where *n* represents the length of the ODMS tail: LC-14Si ($n = 5$), LC-22Si ($n = 9$), LC-30Si ($n = 13$).

marked by sharp order–disorder transitions. None of the compounds are found to crystallize. The room-temperature LC phases were further investigated by bulk X-ray diffraction (XRD) in both wide-angle and medium-angle configurations (Figure 1). For each liquid crystal, two broad peaks were observed in the wide-angle region ($5\ \text{nm}^{-1} < q > 20\ \text{nm}^{-1}$). The first, at $q = 9\ \text{nm}^{-1}$ ($d = 0.70$ nm), is assigned to the mean distance between siloxane units.[17] The second, at $q = 13.4\ \text{nm}^{-1}$ ($d = 0.45$ nm), is assigned to the mean distance between the aliphatic and aromatic parts of the molecule. The presence of two distinct wide angle peaks evidences the nanophase separation between the ODMS and organic molecular components. The medium angle reflections ($1\ \text{nm}^{-1} < q > 5\ \text{nm}^{-1}$) (Table S1, Supporting Information) were used to assign the LC lattice parameters indicated in Figure 1. LC-14Si forms a rectangular columnar phase ($a = 3.8$ nm, $b = 7.4$ nm) (plane group c2nm). LC-22Si also forms a rectangular columnar phase ($a = 4.3$ nm, $b = 8.5$ nm) with a comparatively larger lattice. LC-30Si forms a hexagonal columnar phase ($a = 5.1$ nm) (plane group p6nm). This finding indicates the modularity of the LC approach, i.e., the pitch can be tuned by changing the length of the ODMS tail. Schematic representations of the liquid crystal phases are included in Figure 1. In the columnar phases, the LC cylinder can be considered to consist of an arrangement of rigid rods with a cross section of ≈2.4 nm[20] (red), while the matrix consists of flexible ODMS coils which fill the space between the cylinders[21] (blue). The absence of an "interdisc distance" in the wide-angle region reveals that the rigid cores are relatively unordered within the LC cylinders. The morphology change from the higher-order rectangular columnar phase to the lower-order hexagonal columnar phase is considered a consequence of the increased coil-to-rod volume fraction[21,22] in the LC series.

In order to study the morphology of the LCs in thin films, solutions of LC were spin-coated on Si wafers modified with a PDMS polymer brush.[3] Solutions of 1 wt% in heptane resulted in 40 nm thin films on top of a 4.5 nm brush layer, according to ellipsometry. Atomic force microscopy (AFM)

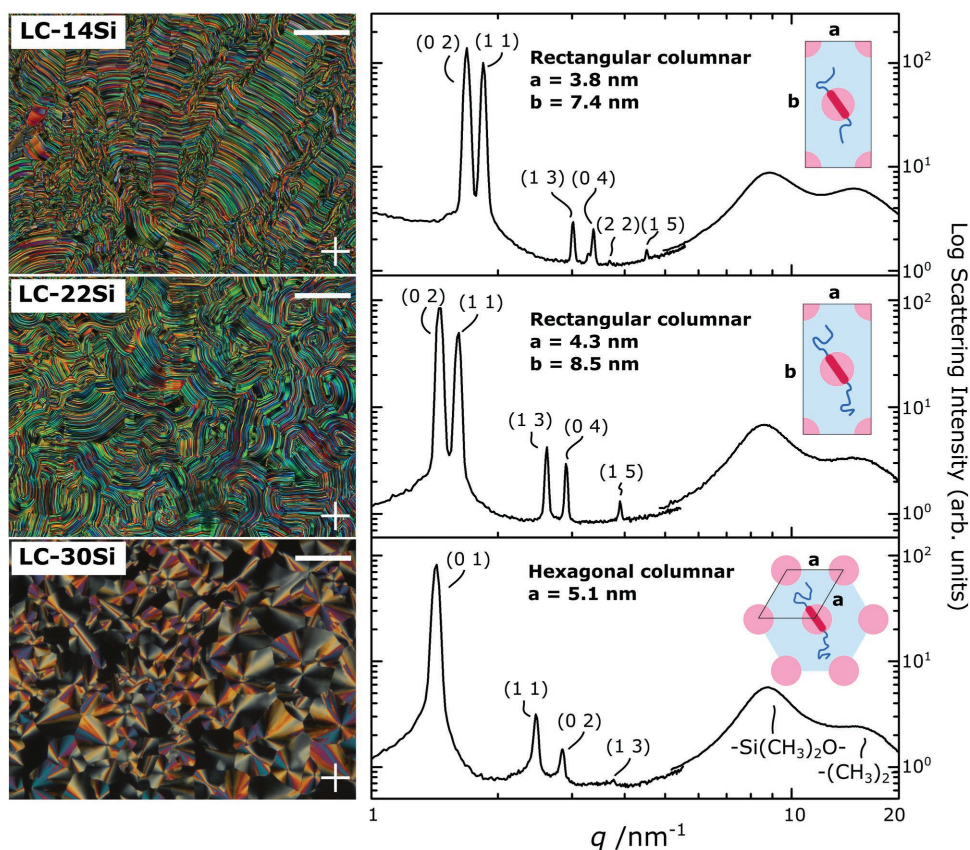

Figure 1. Room-temperature POM images of the ODMS liquid crystals and their corresponding XRD spectra. The POM images were obtained under crossed polarizers (polarizer axes are indicated in the images with a cross). All scale bars: 100 µm. The XRD spectra were collected in both wide- and medium-angle configurations (the transition is marked by a discontinuity at $q \approx 5\ \text{nm}^{-1}$). The assigned Miller indices and the respective intermolecular scatterings are indicated as well as the corresponding lattices.

© 2016 The Authors. Published by WILEY-VCH Verlag GmbH & Co. KGaA, Weinheim

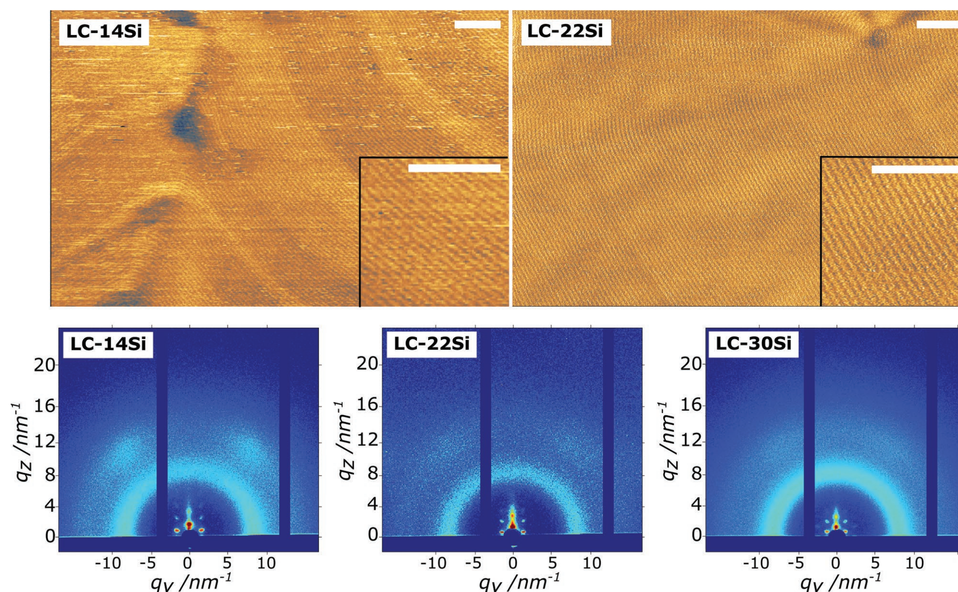

Figure 2. Characterization of as-cast ODMS LC thin films of thickness 40 nm. Top: AFM phase images exhibit line structures produced by in-plane LC cylinders (bright domains). The samples have a period of 3.8 nm (LC-14Si) and 4.3 nm (LC-22Si). Scale bars: 50 nm. Bottom: Grazing-incidence X-ray diffraction data, measured around the critical angle, show the LC phases are maintained in the thin film state and organize preferentially in a planar fashion.

height images reveal that very smooth films are obtained (Figure S3, Supporting Information). AFM phase images of the thin films surface exhibit highly ordered line features indicative of a planar orientation of LC cylinders (**Figure 2**). Since the surface energy of the ODMS tails is presumed to be very low (γ_{PDMS} = 20.5 mN m^{-1}),[23] the siloxane tails are anticipated to wet the air interface. Since the cylinder structures are buried inside the film, the contrast in AFM height and phase images is assumed to arise from the disparate mechanical properties of the rigid LC core and flexible ODMS tails in tapping mode (core = light, ODMS = dark). The center-to-center distances were determined by Fourier analysis. For the columnar rectangular phases of LC-14Si and LC-22Si, distances of 3.8 and 4.3 nm are found, respectively, corresponding to lattice parameter "*a*" in each case. Lattice parameter "*b*" was not seen, suggesting a preferential orientation of the columnar lattice with "*a*" parallel to the substrate and "*b*" perpendicular to the substrate. The defect density in these as-cast, unannealed films is remarkably low. At the same time, the orientation of the microdomains is preserved over large distances, indicating a naturally large correlation length between the LC cylinders, in accordance with POM observations of bulk material. Grazing-incidence XRD was performed in both wide-angle (Figure 2) and medium-angle (Figure S4, Supporting Information) configurations to investigate the through-film morphology of the thin films. In line with bulk measurements, the broad reflections at 7 nm^{-1} < q < 14 nm^{-1} signify that the liquid-like nature of the respective intermolecular interactions (siloxane–siloxane and organic–organic) is maintained in the thin films. The medium-angle reflections are collected in Table S2 (Supporting Information) and were used to assign the LC lattice parameters. The observed distinct Bragg spots confirm the LC cylinders are oriented parallel to the substrate. For LC-14Si, the scattering data are fitted with a rectangular lattice (a = 3.8 nm, b = 7.4 nm, plane group c2nm). For LC-22Si, the scattering data are fitted with a rectangular lattice (a = 4.3 nm, b = 8.5 nm, plane group c2nm). The rectangular lattices are oriented with their short axis "*a*" parallel to the surface, in line with AFM observations. For LC-30Si, the scattering data are fitted with a hexagonal lattice (a = 5.1 nm, plane group p6nm). In each case, the presence of higher order reflections is a sign of the high lateral order and large correlation lengths, in accordance with AFM. We argue that the LC nature of the film and absence of polydispersity are responsible for the high lateral order. Interestingly, the bulk and thin film periodicities correspond exactly. This finding stands in contrast with thin block copolymer films, where the periodicity typically increases by ≈10% from the bulk due to stretching of the polymer chains.[5,24]

We further investigated the directed self-assembly of the LC in graphoepitaxial trenches of ≈100 nm in width, which were patterned with classical 193 nm immersion lithography and modified with a PDMS polymer brush. The patterned wafers were coated with a 1 wt% heptane solution of LC-22Si. AFM reveals multilayers confined inside the trenches with the cylindrical long axis parallel to the trench walls (**Figure 3**). The trench is subdivided into 24 smaller line structures with a 4.3 nm periodicity (obtained from Fourier analysis). The high order is remarkable considering the absence of any annealing or further optimization of any kind and clearly demonstrates the potential of using liquid crystals for the production of monolithic systems. However, the lithographic processes used to produce the trenches are imperfect which results in local variations of the trench width on the order of several nanometers.[25] Apparent defects result from confinement of the LC by trench walls with nonzero roughness, which causes bending of the line structures, in addition to a few disclinations; however, these largely limited to the edge of each channel.[26] Given the low density of nonequilibrium defects in samples with no

© 2016 The Authors. Published by WILEY-VCH Verlag GmbH & Co. KGaA, Weinheim

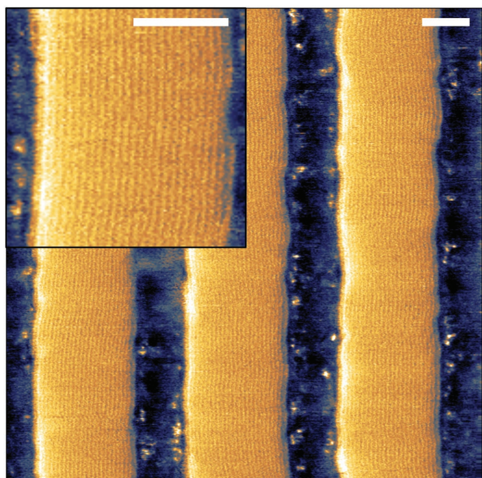

Figure 3. AFM phase images of as-cast LC-22Si thin films within graphoepitaxial trenches of ≈100 nm width. Highly ordered line structures are formed with a period of 4.3 nm. The inset corresponds to a 2× magnification. Scale bars: 50 nm.

directing features (≈2 defects μm^{-2}, based on Figure 2 and similar images), it is unlikely that such defects are present within the trenches. Other apparent defects are likely artifacts due to a combination of noise and row misalignment, given the small periodicity (4.3 nm) relative to the AFM resolution (1 pixel nm^{-1}). Furthermore, the LC periodicity does not fluctuate as it is fixed by the LC lattice parameters, and hence, the placement error is on the order of the trench roughness.[27] The directed self-assembly was also investigated in a wider trench of ≈250 nm in width (Figure S5, Supporting Information). In this case, the line structures no longer align perfectly to the prepattern, indicating that the influence of the trench walls is insufficient to sustain lateral ordering across the breadth of the trench.

Here, we have introduced oligo(dimethylsiloxane) liquid crystals as candidates for sub-5 nm nanopatterning. The ease with which these materials align by graphoepitaxial templates bears witness to the benefit of using liquid crystals for obtaining ultrasmall, highly ordered nanopatterns. In perspective, the use of liquid crystals could provide a real advantage over block copolymers not only in feature size but also by the lack of variations in domain size and periodicity in thin films versus bulk and across a trench.[28] For pattern registration, however, further roughness reduction could be achieved with an optimized photolithographic step or by a next generation extreme-UV lithographical tool.

The next steps toward liquid crystal based nanolithography are first, the casting of single layer films, and then pattern transfer of the ODMS nanopatterns by etching. Preliminary experiments show that uniform thin films can be prepared in which the LC morphology is maintained by adjusting the spin-coating concentration (Figures S6, S7, and S8, Supporting Information). Furthermore, oxygen plasma etching experiments on a multilayer film indicate that the organics are etched away while the ODMS is oxidized (Figure S9, Supporting Information), demonstrating the potential of these liquid crystals for nanolithography. It must however be stressed that the optimization of etching parameters for pattern transfer will be a nontrivial exercise considering the limited aspect ratio of the in-plane cylinders in combination with the sub-5 nm dimensions. In this context, an out-of-plane orientation of cylinders would be desirable, which could be achieved by tuning the chemistries at the interfaces.[29]

Experimental Section

LC Synthesis: Oligo(dimethylsiloxane)s were prepared by coupling a linear trisiloxane to a linear chlorotetrasiloxane in an iterative fashion,[18] producing a heptasiloxane monohydride (first cycle), an undecasiloxane monohydride (second cycle), and pentadecasiloxane (third cycle). A rigid core was synthesized by reaction of 4-(butenyloxy)benzoic acid with 4,4′-dihydroxy azobenzene in an esterification reaction with dicyclohexylcarbodiimide and 4-dimethylaminopyridine.[19] Subsequently, the respective oligo(dimethylsiloxane) hydrides were coupled to the core, using Karstedt's catalyst, as detailed in the Supporting Information.

POM Measurements: A small amount of LC material was placed between microscope slides, heated to the isotropic phase, and cooled (10 °C min^{-1}) to room temperature by a hot stage (Linkam, THMS600) coupled to a polarized optical microscope (POM) (Leica DM6000M), equipped with a DFC420C camera.

X-Ray Measurements: X-ray scattering measurements were performed on a Ganesha lab instrument equipped with a GeniX-Cu ultralow divergence source producing X-ray photons with a wavelength of 1.54 Å and a flux of 1 × 10^{8} ph s^{-1}. Scattering patterns were collected using a Pilatus 300 K silicon pixel detector. The beam center and the q range were calibrated using the diffraction peaks of silver behenate. Bulk XRD was performed on samples sealed in a 1 mm glass capillary. Grazing incidence XRD was performed at the critical angle (≈0.18°). The sample to detector distance was 91 mm for wide-angle measurements and 441 mm for medium-angle measurements.

AFM Measurements: The AFM data were recorded in ambient conditions using a Dimension ICON atomic force microscope (Bruker Nano Inc., Santa Barbara, CA) fitted with a silicon probe (Bruker, NCHV, spring constant 42 N m^{-1} and a resonance frequency 320 kHz). The AFM images were all captured on films without any etching, so a thin wetting layer of ODMS is presumably at the air–LC interface.

Thin-Film Preparation: A hydroxy-terminated PDMS homopolymer from Polymer Source Inc. with molecular weight 5 kg mol^{-1} was applied onto templated or untemplated silicon substrates from a 1–2 wt% solution in heptane, baked at 150 °C for at least 24 h, and rinsed with heptane. The liquid crystals were subsequently spin coated from 1 wt% solution in heptane (3000 rotations minute^{-1}, 45 s).

Fabrication of Trenches: Spin-on carbon (SOC) HM710 and spin-on glass (SOG) ISX304 from JSR Micro were used with vendor recommended process conditions. Negative tone development photoresist AN02 from FUJIFILM was patterned on this stack using an ASML NXT:1950i ArF immersion scanner with moderate off-axis illumination conditions (numerical aperture 1.2, annular illumination, $\sigma_o/\sigma_i = 0.8/0.6$). The resist patterns were transferred into the SOC using a Tokyo Electron Limited (TEL) Tactras dry etch system and the SOG was removed using 0.5% Hydrofluoric acid on a TEL CELLESTA wafer clean system.

Plasma Etching: Oxygen plasma etching was performed with an Emitech K1050X RF plasma reactor operating in plasma ashing mode. The X-ray photoelectron spectrscopy (XPS) measurements were carried out with a Thermo Scientific K-Alpha, equipped with a monochromatic small-spot X-ray source and a 180° double focusing hemispherical analyzer with a 128-channel detector. The spectra were obtained using an aluminum anode (Al Kα = 1486.6 eV) operating at 72 W and a spot size of 400 μm.

Ellipsometry: Ellipsometric measurements were acquired via nulling ellipsometry using a spectroscopic imaging ellipsometer (Accurion Nanofilm ep4, Accurion GmbH, Göttingen, Germany) fit with a 10× objective (≈2 μm lateral resolution). Data were collected at angles

© 2016 The Authors. Published by WILEY-VCH Verlag GmbH & Co. KGaA, Weinheim

from 50° to 70° at selected wavelengths from 350 to 1000 nm. The data were modeled based on sequential measurements of the thermal oxide (≈2 nm) on Si⟨100⟩, the PDMS brush (≈5 nm), and various layers of LC-22Si.

Supporting Information

Supporting Information is available from the Wiley Online Library or from the author.

Acknowledgements

The research was made possible by a grant of Technology Foundation STW. The authors thank Ralf Bovee for mass spectrometry measurements, Tiny Verhoeven for XPS measurements, Ilja Voets for XRD support, Sander Wuister and Tamara Druzhinina from ASML for general support, and Theo Dingemans and Bert Meijer for discussions. P. Leclère is Senior Research Associate from Fonds de la Recherche Scientifique (FRS-FNRS) (Belgium). The X-ray diffractometer was financed by The Netherlands Organisation for Scientific Research (NWO).

Received: June 1, 2016
Revised: August 21, 2016
Published online: September 30, 2016

[1] a) A. Nunns, J. Gwyther, I. Manners, *Polymer* **2013**, *54*, 1269; b) J. D. Cushen, I. Otsuka, C. M. Bates, S. Halila, S. Fort, C. Rochas, J. A. Easley, E. L. Rausch, A. Thio, R. Borsali, C. G. Willson, C. J. Ellison, *ACS Nano* **2012**, *6*, 3424; c) X. Yu, K. Yue, I. F. Hsieh, Y. Li, X. H. Dong, C. Liu, Y. Xin, H. F. Wang, A. C. Shi, G. R. Newkome, R. M. Ho, E. Q. Chen, W. B. Zhang, S. Z. Cheng, *Proc. Natl. Acad. Sci.USA* **2013**, *110*, 10078.
[2] a) Y. S. Jung, J. B. Chang, E. Verploegen, K. K. Berggren, C. A. Ross, *Nano Lett.* **2010**, *10*, 1000; b) M. L. Wadey, I. F. Hsieh, K. A. Cavicchi, S. Z. D. Cheng, *Macromolecules* **2012**, *45*, 5538; c) C. C. Chao, T. C. Wang, R. M. Ho, P. Georgopanos, A. Avgeropoulos, E. L. Thomas, *ACS Nano* **2010**, *4*, 2088.
[3] Y. S. Jung, C. A. Ross, *Nano Lett.* **2007**, *7*, 2046.
[4] C. Sinturel, F. S. Bates, M. A. Hillmyer, *ACS Macro Lett.* **2015**, *4*, 1044.
[5] Y. Luo, D. Montarnal, S. Kim, W. Shi, K. P. Barteau, C. W. Pester, P. D. Hustad, M. D. Christianson, G. H. Fredrickson, E. J. Kramer, C. J. Hawker, *Macromolecules* **2015**, *48*, 3422.
[6] a) J. W. Jeong, W. I. Park, M.-J. Kim, C. A. Ross, Y. S. Jung, *Nano Lett.* **2011**, *11*, 4095; b) L. M. Pitet, S. F. Wuister, E. Peeters, E. J. Kramer, C. J. Hawker, E. W. Meijer, *Macromolecules* **2013**, *46*, 8289.
[7] M. Luo, T. H. Epps, *Macromolecules* **2013**, *46*, 7567.
[8] H. Pathangi, B. T. Chan, H. Bayana, N. Vandenbroeck, D. Van den Heuvel, L. Van Look, P. Rincon-Delgadillo, Y. Cao, J. Kim, G. Y. Lin, D. Parnell, K. Nafus, R. Harukawa, I. Chikashi, M. Polli, L. D'Urzo, R. Gronheid, P. Nealey, *J. Micro/Nanolithogr. MEMS* **2015**, *14*, 031204.
[9] a) M. Lee, B. K. Cho, Y. G. Jang, W. C. Zin, *J. Am. Chem. Soc.* **2000**, *122*, 7449; b) C. Keith, R. A. Reddy, A. Hauser, U. Baumeister, C. Tschierske, *J. Am. Chem. Soc.* **2006**, *128*, 3051; c) C. Tschierske, *Curr. Opin. Colloid Interface Sci.* **2002**, *7*, 69; d) C. Tschierske, *J. Mater. Chem.* **2001**, *11*, 2647; f) Q. Zhou, T. Chen, J. Zhang, L. Wan, P. Xie, C. C. Han, S. Yan, R. Zhang, *Tetrahedron Lett.* **2008**, *49*, 5522; g) M. Zhou, T. J. Kidd, R. D. Noble, D. L. Gin, *Adv. Mater.* **2005**, *17*, 1850; h) X. D. Feng, M. E. Tousley, M. G. Cowan, B. R. Wiesenauer, S. Nejati, Y. Choo, R. D. Noble, M. Elimelech, D. L. Gin, C. O. Osuji, *ACS Nano* **2014**, *8*, 11977.
[10] R. H. Zha, B. F. de Waal, M. Lutz, A. J. Teunissen, E. W. Meijer, *J. Am. Chem. Soc.* **2016**, *138*, 5693.
[11] a) T. Seki, S. Nagano, M. Hara, *Polymer* **2013**, *54*, 6053; b) A. Natansohn, P. Rochon, *Chem. Rev.* **2002**, *102*, 4139; c) T. Ikeda, *J. Mater. Chem.* **2003**, *13*, 2037.
[12] J. C. Wittmann, P. Smith, *Nature* **1991**, *352*, 414.
[13] J. Cattle, P. Bao, J. P. Bramble, R. J. Bushby, S. D. Evans, J. E. Lydon, D. J. Tate, *Adv. Funct. Mater.* **2013**, *23*, 5997.
[14] P. O. Mouthuy, S. Melinte, Y. H. Geerts, A. M. Jonas, *Nano Lett.* **2007**, *7*, 2627.
[15] a) C. V. Cerclier, M. Ndao, R. Busselez, R. Lefort, E. Grelet, P. Huber, A. V. Kityk, L. Noirez, A. Schonhals, D. Morineau, *J. Phys. Chem. C* **2012**, *116*, 18990; b) R. B. Zhang, X. B. Zeng, B. Kim, R. J. Bushby, K. Shin, P. J. Baker, V. Percec, P. Leowanawat, G. Ungar, *ACS Nano* **2015**, *9*, 1759.
[16] a) C. Pugh, J. Y. Bae, J. Dharia, J. J. Ge, S. Z. D. Cheng, *Macromolecules* **1998**, *31*, 5188; b) L. Wang, Y. Ishida, R. Maeda, M. Tokita, S. Horiuchi, T. Hayakawa, *Langmuir* **2014**, *30*, 9797; c) E. Nishikawa, E. T. Samulski, *Liq. Cryst.* **2000**, *27*, 1457.
[17] C. Keith, R. A. Reddy, U. Baumeister, C. Tschierske, *J. Am. Chem. Soc.* **2004**, *126*, 14312.
[18] B. van Genabeek, B. F. M. de Waal, M. M. J. Gosens, L. M. Pitet, A. R. A. Palmans, E. W. Meijer, *J. Am. Chem. Soc.* **2016**, *138*, 4210.
[19] a) J. Garcia-Amoros, A. Szymczyk, D. Velasco, *Phys. Chem. Chem. Phys.* **2009**, *11*, 4244; b) A. Sanchez-Ferrer, A. Merekalov, H. Finkelmann, *Macromol. Rapid Commun.* **2011**, *32*, 671.
[20] J. Garcia-Amoros, A. Szymczyk, D. Velasco, *Phys. Chem. Chem. Phys.* **2009**, *11*, 4244.
[21] M. Lee, B. K. Cho, H. Kim, J. Y. Yoon, W. C. Zin, *J. Am. Chem. Soc.* **1998**, *120*, 9168.
[22] E. Nishikawa, E. T. Samulski, *Liq. Cryst.* **2000**, *27*, 1463.
[23] S. Wu, *Polymer Handbook*, Vol. *VI*, Wiley-Interscience, New York **1989**.
[24] K. Aissou, M. Mumtaz, G. Fleury, G. Portale, C. Navarro, E. Cloutet, C. Brochon, C. A. Ross, G. Hadziioannou, *Adv. Mater.* **2015**, *27*, 261.
[25] B. Kim, N. Laachi, K. T. Delaney, G. H. Fredrickson, *Proc. SPIE* **2014**, *9049*, 90491D.
[26] a) Q. Tong, Q. Zheng, S. J. Sibener, *Macromolecules* **2014**, *47*, 4236; b) J. Chai, J. M. Buriak, *ACS Nano* **2008**, *2*, 489.
[27] a) S. G. Xiao, X. M. Yang, *J. Vac. Sci. Technol. B* **2007**, *25*, 1953; b) H. Boots, J. M. de Ruiter, T. T. Nguyen, A. Brizard, E. Peeters, S. F. Wuister, T. S. Druzhinina, J. K. Wolterink, J. G. E. M. Fraaije, *J. Micro/Nanolithogr. MEMS* **2014**, *13*, 033015; c) J. Y. Cheng, A. M. Mayes, C. A. Ross, *Nat. Mater.* **2004**, *3*, 823.
[28] T. Graves, A. V. Pret, S. Robertson, M. Smith, J. Doise, J. Bekaert, R. Gronheid, *Proc. SPIE* **2015**, *9425*, 94250Y.
[29] a) C. M. Bates, T. Seshimo, M. J. Maher, W. J. Durand, J. D. Cushen, L. M. Dean, G. Blachut, C. J. Ellison, C. G. Willson, *Science* **2012**, *338*, 775; b) E. Kim, W. Kim, K. H. Lee, C. A. Ross, J. G. Son, *Adv. Funct. Mater.* **2014**, *24*, 6981; c) J. G. Son, K. W. Gotrik, C. A. Ross, *ACS Macro Lett.* **2012**, *1*, 1279.

© 2016 The Authors. Published by WILEY-VCH Verlag GmbH & Co. KGaA, Weinheim